



Effect of amine functionalization of spherical MCM-41 and SBA-15 on controlled drug release

A. Szegedi^{a,*}, M. Popova^b, I. Goshev^b, J. Mihály^a

^a Institute of Nanochemistry and Catalysis, Chemical Research Center, Hungarian Academy of Sciences, 1025 Budapest, Pusztaszeri út 59-67, Hungary

^b Institute of Organic Chemistry with Centre of Phytochemistry, Bulgarian Academy of Sciences, Sofia, Bulgaria

ARTICLE INFO

Article history:

Received 17 November 2010

Received in revised form

10 February 2011

Accepted 3 March 2011

Available online 21 March 2011

Keywords:

Mesoporous silica

Drug release

Ibuprofen

ABSTRACT

MCM-41 and SBA-15 silica materials with spherical morphology and different particle sizes were synthesized and modified by post-synthesis method with 3-aminopropyltriethoxysilane (APTES). A comparative study of the adsorption and release of a model drug, ibuprofen, were carried out. The modified and drug loaded mesoporous materials were characterized by XRD, TEM, N₂ physisorption, thermal analysis, elemental analysis and FT-IR spectroscopy. Surface modification with amino groups resulted in high degree of ibuprofen loading and slow rate of release for MCM-41, whereas it was the opposite for SBA-15. The adsorbed drug content and the delivery rate can be predetermined by the choice of mesoporous material with the appropriate structural characteristics and surface functionality.

© 2011 Elsevier Inc. All rights reserved.

1. Introduction

Recently, there has been increased interest in mesoporous silica materials applied as drug carriers in the field of controlled drug release, to meet the need for prolonged and better control of drug administration [1–16]. Mesoporous silica nanoparticles with a high BET surface area, large pore volume, uniform porosity, stable aqueous dispersion, excellent biocompatibility, in vivo biodegradability, and their capability to be functionalized with different organic groups, are attractive candidates for a wide range of biomedical purposes, such as controlled drug delivery, bone tissue regeneration, cell tracking and immobilization of proteins or enzymes. They have been proposed for the first time as carriers for drug delivery in 2001 by Vallet-Regí et al. [1]. Mesoporous materials also fulfill the conditions for homogenous distribution of the drug through the matrix in contrast to the conventionally used polymeric materials [17–31]. Several key factors should be considered when designing these systems. The pore size of the mesoporous materials to host the guest drug molecules determines the size of the molecule to be adsorbed into the mesopores. Hence, the adsorption and release of drug molecules in the mesoporous matrix are governed by size selectivity. Another factor to be considered in the development of drug delivery system is the chemical relationship between drug molecules and the mesopore wall. The presence of numerous superficial silanol groups makes the surface modification with the appropriate organic group depending on the host

molecule possible. The appropriate chemical modification of the silanol groups should enhance the adsorption and confinement of drug molecules and it should also allow modulating their release. An analgesic and anti-inflammatory drug, ibuprofen was chosen as a model molecule. Ibuprofen can be impregnated into mesoporous silica materials by reacting with the active groups on the mesoporous framework, for instance, by hydrogen bond with surface silanol groups. Amine-functionalized spherical MCM-41 with particle size of 490–770 nm has been investigated by Manzano et al. [17] as carriers of ibuprofen. The results show increased loading capacity (by about 10%) and slower drug release kinetics for amino-modified samples in comparison to the MCM-41 with irregular particle size and shape. The modification of MCM-41 by different organic groups (chloropropyl, phenyl, benzyl, mercaptopropyl, cyanopropyl, and butyl groups) shows higher ibuprofen loading for the polar groups and the ibuprofen release is slowed down with SH-Pr and NH₂-Pr groups [15]. The novel mesoporous silica material TUD-1 shows high amount of adsorbed ibuprofen (drug/carriers 49.5 wt%) [27], with fast release properties. The highest storage amount of 969 mg/g has been obtained by hollow mesoporous sphere with cubic pore network as a carrier of ibuprofen [28], but with faster release rate in comparison to its amino-modified analogs. To the best of our knowledge no data are available for application of the spherical SBA-15 as drug carrier as well as spherical MCM-41 with nanosized particles below 400 nm.

The aim of this work is to investigate the influence of the structural characteristics (pore and particle size) and the chemical interaction of drug-matrix on the insertion and delivery of ibuprofen in amino-modified mesoporous spherical MCM-41 and spherical SBA-15 silica materials.

* Corresponding author.

E-mail address: szegedi@chemres.hu (A. Szegedi).

2. Experimental

2.1. Synthesis of spherical MCM-41 and SBA-15 silica materials

The parent MCM-41 and SBA-15 materials were synthesized by the procedures described in [32,33] and [34], respectively.

MCM-41 material with spherical morphology and larger particle sizes was synthesized by the sol-gel, room-temperature procedure of Grün et al. [32], applying the modified Stöber synthesis of monodispersed silica spheres, using N-hexadecyltrimethyl-ammoniumbromide ($C_{16}TMABr$) as template, tetraethylorthosilicate (TEOS) as silica source and ethanol as co-solvent. The relative molar composition of the synthesis mixture was: 1TEOS:0.3 $C_{16}TMABr$:11 NH_3 :144 H_2O : 58EtOH. The formed gel was aged 2 h at room temperature with stirring and 16 h without it. The product was washed with distilled water until neutral pH was reached, and dried at ambient.

MCM-41 with 100 nm particle size was prepared according to the procedure of Huh et al. [33]. This sol-gel procedure is carried out at 353 K without co-solvent, only in water solution and NaOH as a catalyst. The relative molar composition of the reaction mixture was: 1TEOS:0.12 $C_{16}TMABr$:0.31NaOH:1190 H_2O . The formed gel was aged at 353 K for 2 h, than washed with distilled water until neutral pH, and dried at ambient. Template removal of MCM-41 materials was carried out in air at 823 K with 1 K/min rate for 5 h.

Spherical SBA-15 was synthesized by the procedure of Katiyar et al. [34]. Pluronic P123 (triblockcopolymer (PEO₂₀PPO₇₀PEO₂₀)), and $C_{16}TMABr$ were used as templates and TEOS as silica source. The synthesis media contained also ethanol beside the usual HCl solution. Synthesis mixture with the following relative molar composition was applied: 1TEOS:0.012PEO₂₀PPO₇₀PEO₂₀:0.036 $C_{16}TMABr$:2HCl:7.6EtOH:44.8 H_2O . The mixture was stirred at 308 K for 45 min than put in a Teflon lined autoclave and aged at 348 K for 10 h and subsequently at 393 K for 36 h. The product was washed chloride free with distilled water and dried at ambient. Template removal was carried out in air at 723 K with 1 K/min rate for 5 h.

The parent mesoporous spherical silica materials were designated as MCM-41(s) or MCM-31(l) and SBA-15(l) and the particle size is denoted in the parentheses as (s)—for small particle, below 1 μm and (l) – for large particle, above 1 μm .

2.2. Modification of the materials by APTES

Modification of the spherical MCM-41 and SBA-15 materials with amino groups was accomplished by reaction with 3-aminopropyltriethoxysilane (APTES) (24 h, 333 K) in toluene. After that the reaction materials were washed with several portions of toluene, methanol, and finally water. For MCM-41, 1 g of the silica were reacted with 20 ml APTES in 100 ml toluene. For SBA-15, 900 mg of the silica were reacted with 12 ml of APTES in 30 ml of toluene. The amino-modified materials were dried at room temperature.

The modified samples by APTES were designated as MCM-41(s) NH_2 , MCM-41(l) NH_2 and SBA-15(l) NH_2 .

2.3. Characterization

X-ray diffractograms were recorded by a Philips PW 1810/3710 diffractometer with Bregg–Brentano parafocusing geometry applying monochromatized $CuK\alpha$ ($\lambda=0.15418$ nm) radiation (40 kV, 35 mA) and proportional counter.

Nitrogen physisorption measurements were carried out at 77 K using Quantachrome NOVA Automated Gas Sorption Instrument. The pore-size distributions were calculated from the desorption

branch of the isotherms with the BJH method. Samples were pre-treated at 353 K for 5 h before measurements.

TEM images were taken using a MORGAGNI 268D TEM (100 kV; W filament; point-resolution=0.5 nm).

The thermogravimetric measurements were performed with a Setaram TG92 instrument with a heating rate of 5 K/min in nitrogen flow.

Carbon, hydrogen and nitrogen contents of the samples were determined using a Vario EL III CHNOS elemental analyzer.

FT-IR spectrum was recorded in KBr pellets (99 wt% of KBr) on a Bruker Vector 22 spectrophotometer.

2.4. Ibuprofen loading and in-vitro release measurements

Powdered mesoporous samples were loaded with ibuprofen by soaking them, under continuous magnetic stirring for 24 h at 310 K, into a hexane solution of ibuprofen. A 1:1 (by weight) ratio of ibuprofen to solid sample was used. In practice 150 mg of ibuprofen was dissolved in 5 ml of hexane and 150 mg of dried mesoporous silica was put into this solution. Ibuprofen loaded samples were recovered by filtration, washed with hexane and dried for 24 h at 313 K. In-vitro drug release experiment was performed as follows: a disk (60 mg) of pressed drug storage material was immersed into 60 ml simulated body fluid (SBF) of pH=7.4 at 313 K, under stirring at a rate of 200 min^{-1} . 2 ml extracted solution was analyzed with UV-vis spectroscopy at a wavelength of 264 nm.

3. Results and discussion

3.1. Material characterization

Formation of spherical MCM-41 materials with particle sizes of 100 nm and 1 μm was evidenced by TEM measurements (Fig. 1A and B). Spherical SBA-15 with particles of 5 μm was obtained (Fig. 1C) and it was applied as drug carriers for the first time.

XRD data of the spherical MCM-41(s), MCM-41(l) and SBA-15(l) samples (not shown) with the intense (1 0 0) and higher Miller indices reflections in the low 2θ region confirm the formation of the hexagonal structure. However, some broadening and shifting of the diffraction peaks are observed for the amino-modified and ibuprofen loaded mesoporous samples, indicating the decrease in structural order.

The nitrogen adsorption and desorption isotherms of all parent, amino-modified and ibuprofen loaded samples are presented in Fig. 2 and the calculated textural parameters are presented in Table 1. The isotherms of the initial MCM-41(s) and MCM-41(l) modifications exhibit a sharp increase at a relative pressure of $p/p_0=0.2-0.4$, which is associated with capillary condensation in the channels and narrow pore size distribution (Fig. 2). The position of this step can be found at higher relative pressure for the SBA-15(l) sample (Fig. 2) indicating the presence of larger size pores (Table 1). The isotherms of the MCM-41(s), (l) samples are reversible and do not show any hysteresis loop whereas the isotherms of the SBA-15(l) exhibit a H2 type hysteresis loop, which is a typical feature for this type of mesoporous material. A significant decrease in BET surface area, pore volume and pore size is observed for the amino-modified MCM-41(s), (l) and SBA-15(l) materials (Table 1). This decrease is more significant for the MCM-41(l) sample. The pore structure of the latter sample seems to be more sensitive to amino-modification resulting in partial collapse of the channel system. This can either be due to the different channel systems of the two MCM-41 preparations (see TEM images) or the condensation degree of silanol groups

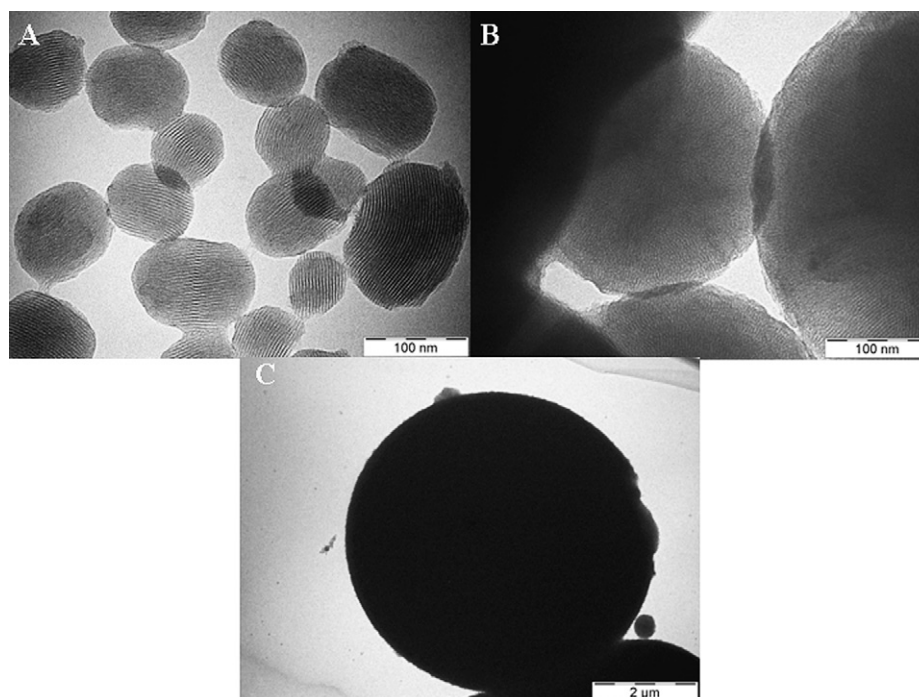


Fig. 1. TEM images of (A) MCM(s), (B) MCM-41(l) and (C) SBA-15(l) materials.

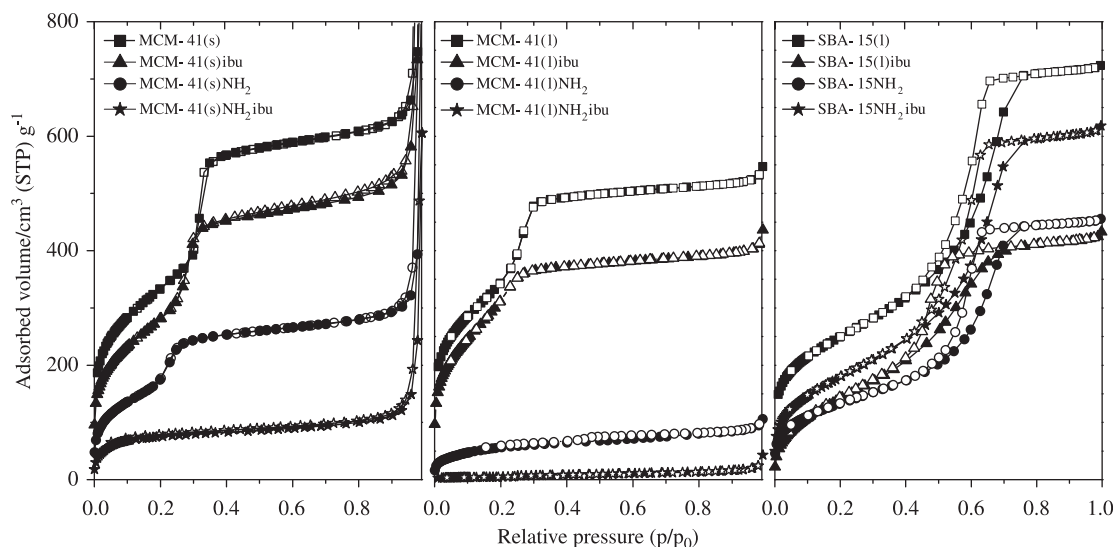


Fig. 2. Nitrogen adsorption/desorption isotherms of the parent, the amino-modified and ibuprofen loaded MCM-41(s), MCM-41(l) and SBA-15(l) materials.

originating from the different preparation procedures (room temperature for MCM-41(l) and 310 K for MCM-41(s) material). MCM-41(s) has straight channels crossing the entire particle and lower amount of hydrogen bonded silanol groups on the surface evidenced by the lower weight loss in TG curve over 773 K (not shown). The particles of the spherical MCM-41(l) are built of a core with cubic structure and a shell, which consists of channels radially orientated toward the center of the particle (Fig. 1A) [35]. The structure is built up of domains of parallel short channels separated by thicker walls and the lower condensation of silanol groups is a consequence of the room temperature synthesis method.

The textural parameters of the parent MCM-41 samples loaded with ibuprofen show some decrease in the surface area, pore diameter, and pore volume, but the pores are not filled entirely (Table 1). The amino-modified MCM-41(s) material exhibits pore filling after the interaction with ibuprofen solution (Fig. 2 and

Table 1). The adsorption of ibuprofen on MCM-41(l) is related to extreme decrease of specific surface area, because of the total pore filling of the disordered pore structure.

Ibuprofen loaded parent SBA-15(l) shows significant decrease of surface area and pore diameter. Ibuprofen adsorption on amino-modified SBA-15 sample results in increased surface area and pore diameter compared to the amino-modified variety. This can be explained by the partial removal of amino-groups from the surface of channels during the ibuprofen loading procedure. Analyzing the N_2 adsorption isotherms by the α_s plot method, the microporous volume of the parent SBA-15(l) sample was $0.05 \text{ cm}^3/\text{g}$. Loading the sample with ibuprofen results in the total filling of micropores due to the appropriate size of drug molecule ($1 \text{ nm} \times 0.5 \text{ nm}$). The modified SBA-15(l) NH_2 sample does not show any presence of micropores, probably because of the interaction of silanol groups inside the micropores with APTES

Table 1
Physicochemical properties and ibuprofen storage and release capacity of the parent and amino-modified spherical MCM-41(s), (l) and SBA-15(l) samples.

Samples	a_0 (nm) ^a	Wall thickness (nm)	BET (m ² /g)	PD (nm) ^b	Pore volume (cm ³ /g)	Adsorbed ibuprofen (mg/g _{ads}) ^c	Released ibuprofen (mg/g _{ads}) ^d
MCM-41(s)	4.43	1.73	1175	2.7	0.987	–	–
MCM-41(s)ibu	4.37	1.87	968	2.5	0.852	151	143
MCM-41(s)NH ₂	4.21	2.01	570	2.2	0.468	–	–
MCM-41(s)NH ₂ ibu	4.32	–	295	n.d.	0.187	368	346
MCM-41(l)	4.16	1.76	1167	2.4	0.825	–	–
MCM-41(l)ibu	4.12	2.02	1049	2.1	0.637	148	139
MCM-41(l)NH ₂	4.12	–	202	n.d.	0.147	–	–
MCM-41(l)NH ₂ ibu	4.12	–	20	n.d.	0.037	314	299
SBA-15	10.22	4.72	878	5.5	1.116	–	–
SBA-15ibu	10.20	6.5	491	3.7	0.659	349	320
SBA-15NH ₂	10.09	4.99	477	5.1	0.701	–	–
SBA-15NH ₂ ibu	9.99	4.59	627	5.4	0.946	177	162

^a Cell parameter ($a_0 = 2d_{100}(3)^{-1/2}$).

^b Pore diameter and pore volume calculated by BJH method (desorption branch).

^c Calculated from TG analysis.

^d Calculated from UV absorbance analysis.

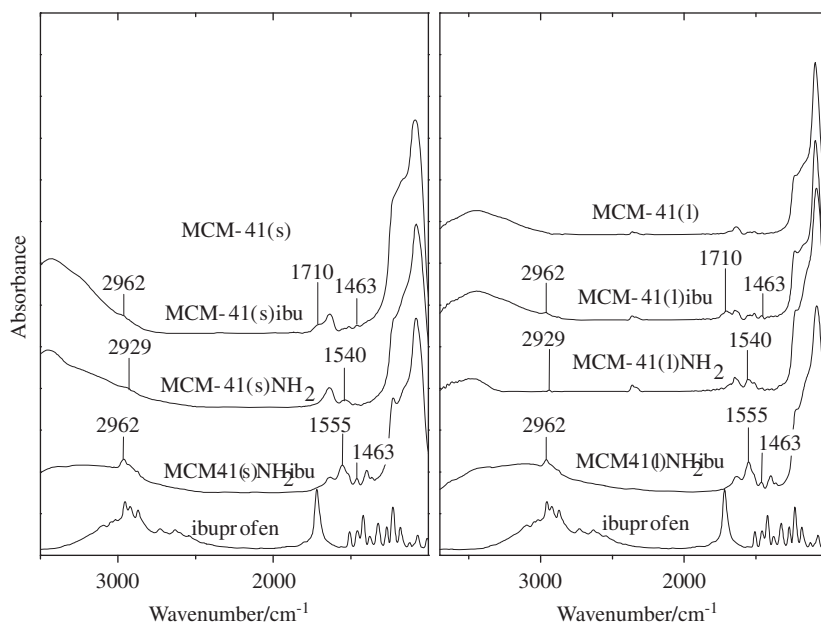


Fig. 3. FT-IR spectra of the parent, the amino-modified and ibuprofen loaded MCM-41(s), (l) materials.

during the modification. Micropores cannot be detected also for ibuprofen loaded sample.

All mesoporous samples were characterized by FT-IR (Figs. 3 and 4), verifying the presence of functional groups after amino-modification and drug adsorption. The asymmetric stretching vibrations (Si–O–Si) appear at about 1090 cm⁻¹ for MCM-41 and at 1075 cm⁻¹ for SBA-15. The modification by APTES of MCM-41(s), (l) and SBA-15(l) samples results in the appearance of the bands at 2929 and at 1540 cm⁻¹, which are attributed to C–H and N–H stretching vibrations of aminopropyl anchored on the surface of mesoporous support [29,36]. The FT-IR spectra of ibuprofen-loaded parent samples (Figs. 3 and 4) show the bands at 2962 and 1463 cm⁻¹ characteristic for C–H and phenyl bands, respectively. The band at 1710 cm⁻¹ registered on ibuprofen loaded parent mesoporous silicas is due to the COOH group of the ibuprofen molecule whereas the presence of the band at 1555 cm⁻¹ in the spectra of the amino modified ibuprofen loaded mesoporous silicas (Figs. 3 and 4) is indicative for the formation of a COO⁻–NH₃⁺ bond [29]. Bands at 1463 and 2962 cm⁻¹, typical

for C–H and phenyl groups are also registered in the spectra of ibuprofen loaded amino-modified samples.

The absence of crystalline ibuprofen reflections in the XRD patterns of the loaded mesoporous MCM-41(s), (l) and SBA-15(l) samples demonstrated that washing had removed all the surface loaded ibuprofen. The ibuprofen loaded in the mesopores of MCM-41(s), (l), SBA-15(l) samples, and their amino-modified analogs was quantified using TG. The thermogravimetric analysis determines the actual amount of drug in the supports (Table 1, and Fig. 5), correcting the curves by water and aminopropyl content. The parent spherical MCM-41(s) and MCM-41(l) show lower adsorption capacity for ibuprofen in comparison to their amino-modified analogs. The highest capacity for ibuprofen loading was measured for MCM-41(s)NH₂ (36.8%) and for SBA-15(l) samples (34.9%) (Table 1). Manzano et al. [17] also found an increased adsorption capacity for amino-modified MCM-41 up to 330 mg/g for the mesoporous support with particle size of 615 nm. The amino-modified spherical SBA-15(l) possesses lower capacity for ibuprofen (17.7%). One possible

explanation is that amino groups are removed partially from the surface during the ibuprofen loading as it was suggested on the basis of N_2 physisorption data and elemental analysis (N content after ibuprofen loading is decreased, see Table 2). The number of possible adsorption sites in mesopores is reduced. On the other hand the low capacity can be related to the distribution of adsorption sites, e.g., the location of silanol groups in the mesoporous support. The micropore fraction in total pore volume of SBA-15 depends on the ratio of the pore wall thickness to the pore diameter and can reach up to 40% [37,38], therefore a part of silanols are located in these micropores. As it was shown by nitrogen physisorption (Fig. 2), the modification of SBA-15(l) by APTES leads to the blocking of micropores, more probably because of their filling with amino groups. Therefore they are inaccessible for the ibuprofen adsorption. Elemental analysis was applied for the determination of the changes in the C, H and N content of the amino modified and the ibuprofen loaded initial and the amino modified samples (Table 2). The data show more significant increase in the carbon content after ibuprofen loading on the amino modified MCM-41 samples in comparison to the non

modified ones, which is related to the higher ibuprofen loading. This effect is the opposite for SBA-15(l) which is in good accordance with the TG data.

3.2. Drug delivery

The results of the ibuprofen release from the parent mesoporous silicas and their amino-modifications are plotted in Fig. 6. The concentration of ibuprofen released in SBF at pH=7.4 as a function of time was determined by UV–vis spectroscopy by monitoring the changes in absorbance at wavelength of 264 nm at suitable intervals of time. The ibuprofen release equilibrium rates of MCM-41(s), (l) samples are much faster (1 h) than that of the amino-modified MCM-41(s), (l) silicas (Fig. 6). Hydrogen bonding between ibuprofen and the parent mesoporous silica materials is relatively weak, so the mass transfer of ibuprofen molecules through the channels is controlled by diffusion. According to the literature [1,28] the pore size of the applied mesoporous support influences the release rate. However, the formed $COO^-NH_3^+$ bond between ibuprofen and the functional groups of the amino-modified MCM-41 samples is stronger than that between ibuprofen and silanol groups of the parent silicas. This effect can explain the slower release rates of ibuprofen from both amino-modified MCM-41 samples in comparison to the silica varieties (Fig. 5). Moreover, MCM-41(s) shows slower release in comparison to MCM-41(l). Our XRD N_2 physisorption data show that even ibuprofen loading procedure made the pore structure of MCM-41(l) less ordered, which can explain the faster release rate of ibuprofen. The difference between release rates are more pronounced for amino-modified MCM-41 samples. It seems that the

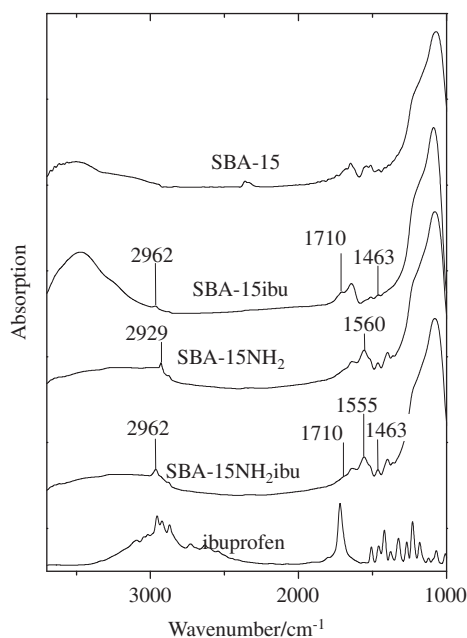


Fig. 4. FT-IR spectra of the parent, the amino-modified and ibuprofen loaded SBA-15(l) materials.

Table 2

Elemental analysis of the parent and amino-modified spherical MCM-41(s), (l) and SBA-15(l) samples before and after ibuprofen loading.

Samples	Element content (wt%)		
	C	H	N
MCM-41(s)ibu	4.5	1.1	0.0
MCM-41(s)NH ₂	6.8	1.6	2.4
MCM-41(s)NH ₂ ibu	21.7	2.9	2.0
MCM-41(l)ibu	2.8	2.2	0.0
MCM-41(l)NH ₂	8.5	2.9	3.1
MCM-41(l)NH ₂ ibu	20.7	3.2	2.8
SBA-15ibu	21.3	1.4	0.0
SBA-15NH ₂	6.3	0.9	2.3
SBA-15NH ₂ ibu	6.3	0.9	0.2

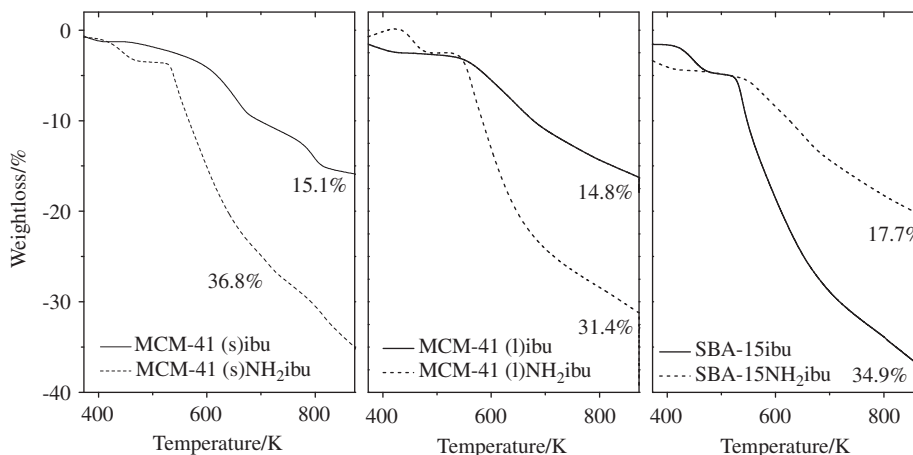


Fig. 5. TG curves of the parent, the amino-modified and ibuprofen loaded MCM-41(s), (l) and SBA-15(l) materials.

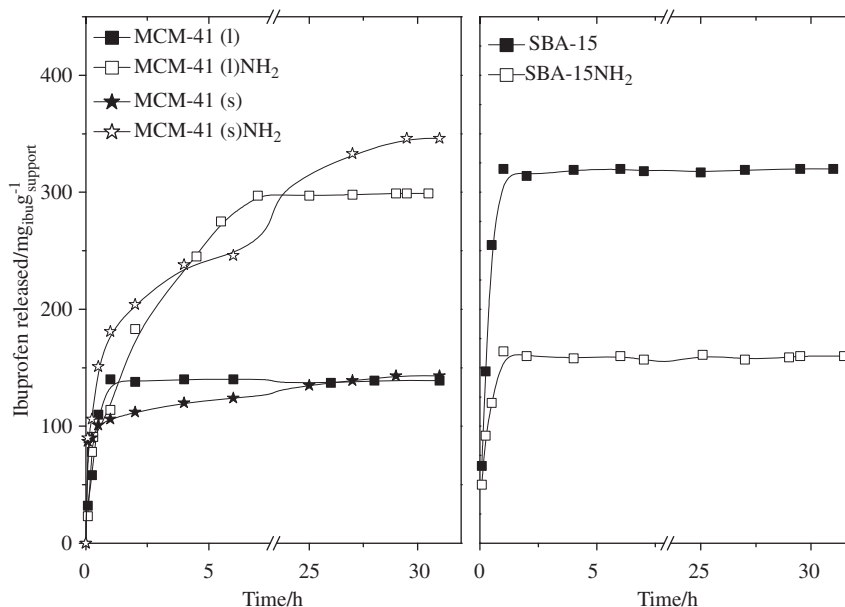


Fig. 6. Ibuprofen delivery from the parent and amino-modified spherical MCM-41(s), (l) and spherical SBA-15(l).

partially collapsed pore structure of amino-modified MCM-41(l) influences more the release rate than the loaded amount of ibuprofen (Table 1 and Fig. 6). Another possible explanation of lower release rate could be the narrower pore size of the mesoporous carriers after modification (see Table 1).

Parent SBA-15(l) shows higher adsorption capacity of ibuprofen than MCM-41 samples, probably due to the higher pore volume (Table 1). The release rate is fast and similar to MCM-41(l). This high adsorption capacity for SBA-15(l) is unique in literature and probably can be associated with the morphology and special channel system of it, e.g., thin walls (Table 1) with short micropore channels which are easy accessible by ibuprofen or organic molecules. In contrast to MCM-41 samples, the amino-modified SBA-15(l) adsorbed lower amount of ibuprofen and the release rate is as fast as it is in the parent one (Fig. 6). As nitrogen physisorption data show, modification of SBA-15(l) with APTES results in blocking the micropores (Fig. 2) where a part of silanol groups is located. Therefore, amino groups in the micropores are inaccessible for ibuprofen and as a result the adsorption capacity of amino modified SBA-15(l)NH₂ is lower. Another aspect is that the mesopore size of SBA-15(l) is larger (about 6 nm) than that of MCM-41 samples (Table 1), and consequently the modification with amino groups of SBA-15(l) cannot significantly hinder the ibuprofen release by diffusion.

4. Conclusion

Spherical MCM-41 and SBA-15 silica materials with different particle sizes were synthesized, modified by amino groups, and studied as carriers for ibuprofen probe molecule. The samples were characterized by XRD and N₂ physisorption, TEM, FT-IR and TG analysis. It revealed that the synthesis procedures of mesoporous MCM-41 materials determine their stability in the surface modification procedure. However, the stability differences did not influence the adsorbed amount of ibuprofen but have significant effect on the release rate. Parent MCM-41 with particle size of 100 nm showed slower release rate. Modification by amino groups had a positive effect on adsorption capacity of ibuprofen in the case of MCM-41 materials. Amino modified MCM-41 with particle size of 100 nm showed the highest adsorption capacity

and slower release rate for ibuprofen in comparison to amino-modified MCM-41 with larger particles. For the first time, spherical SBA-15 was investigated as drug carrier. Its adsorption capacity for ibuprofen with 349 mg/g is very close to the highest value of 368 mg/g obtained by amino-modified MCM-41 with 100 nm particle size. The results showed that the ibuprofen release kinetic can be controlled by the synthesis procedure and the surface functionality of the spherical mesoporous silicas.

Acknowledgment

Financial support by the Nanomedicine project supported by Chemical Research Center of HAS, by the National Office for Research and Technology (GVOP-3.2.1-2004-031163.0), and the Bulgarian-Hungarian Inter-academic Exchange Agreement is greatly acknowledged.

References

- [1] M. Vallet-Regí, A. Ramila, R.P. del Real, J. Perez-Pariente, A new properties of MCM-41: drug delivery system, *Chem. Mater.* 13 (2001) 308–311.
- [2] P. Horcajada, A. Ramia, G. Ferey, M. Vallet-Regí, Influence the superficial modification of MCM-41 matrices on drug delivery rate, *Solid State Sci.* 8 (2006) 1243–1249.
- [3] I.I. Slowing, J.L. Viverro-Escoto, Ch.-W. Wu, V.S.-Y. Lin, Mesoporous silica nanoparticles as controlled release drug delivery and gene transfection carriers, *Adv. Drug Delivery Rev.* 60 (2008) 1278–1288.
- [4] Sh. Wang, Ordered mesoporous materials for drug delivery, *Micropor. Mesopor. Mater.* 117 (2009) 1–9.
- [5] I. Izquierdo-Barba, M. Colilla, M. Manzano, M. Vallet-Regí, *In vitro* stability of SBA-15 under physiological conditions, *Micropor. Mesopor. Mater.* 132 (2010) 442–452.
- [6] X. Huang, X. Teng, D. Chen, F. Tang, J. He, The effect of the shape of mesoporous silica nanoparticles on cellular uptake and cell function, *Biomaterials* 31 (2010) 438–448.
- [7] Q. He, J. Shi, F. Chen, M. Zhu, L. Zhang, An anticancer drug delivery system based on surfactant-templated mesoporous silica nanoparticles, *Biomaterials* 31 (2010) 3335–3346.
- [8] F.J. Trindade, G.J.T. Fernandes, A.S. Araújo, V.J. Fernandes Jr., B.P.G. Silva, R.Y. Nagayasu, M.J. Politi, F.L. Castro, S. Brochsztain, Covalent attachment of 3,4,9,10-perylene diimides onto the walls of mesoporous molecular sieves MCM-41 and SBA-15, *Micropor. Mesopor. Mater.* 113 (2008) 463–471 113 (2008).
- [9] J.M. Rosenholm, M. Linden, Towards establishing-activity relationships for mesoporous silica in drug delivery application., *J. Control. Release* 128 (2008) 157–164.

- [10] P. Yang, Z. Quan, L. Lu, Sh. Huang, J. Lin, Luminescence functionalization of mesoporous silica with different morphologies and applications as drug delivery systems, *Biomaterials* 29 (2008) 692–702.
- [11] G. Wang, A.N. Otuonye, E.A. Blair, K. Denton, Zh. Tao, T. Asefa, Functionalized mesoporous materials for adsorption and release of different drug molecules: a comparative study, *J. Solid State Chem.* 182 (2009) 1649–1660.
- [12] R. Mortera, Sonia Fiorilli, Edoardo Garrone, Enrica Verne, Barbara Onida, Pores occlusion in MCM-41 spheres immersed in SBF and the effect on ibuprofen delivery kinetics: a quantitative model, *Chem. Eng. J.* 156 (2010) 184–192.
- [13] J. Salonen, L. Laitinen, A.M. Kaukonen, J. Tuura, M. Bjoerkqvist, T. Heikkila, K. Vähä-Heikkilä, J. Hirvonen, V.-P. Lehto, Mesoporous silicon microparticles for oral drug delivery: loading and release of five model drugs, *J. Control. Release* 108 (2005) 362–374.
- [14] I. Izquierdo-Barba, A. Martinez, A.L. Doadrio, J. Perez-Pariente, M. Vallet-Regi, Release evaluation of drugs from ordered three-dimensional silica structures, *Eur. J. Pharma. Sci.* 26 (2005) 365–373.
- [15] P. Horcajada, A. Ramila, J. Perez-Pariente, M. Vallet-Regi, Influence of pore size of MCM-41 matrices on drug delivery rate, *Micropor. Mesopor. Mater.* 68 (2004) 105–109.
- [16] Sh. Zhu, Zh. Zhou, D. Zhang, Ch. Jin, Zh. Li, Design and synthesis of delivery system based on SBA-15 with magnetic particles formed in situ and thermo-sensitive PNIPA as controlled switch, *Micropor. Mesopor. Mater.* 106 (2007) 56–61.
- [17] M. Manzano, V. Aina, C.O. Areal, F. Balas, V. Cauda, M. Colilla, M.R. Delgado, M. Vallet-Regi, Studies on MCM-41 mesoporous silica for drug delivery: effect of particle morphology and amine functionalization, *Chem. Eng. J.* 137 (2008) 30–37.
- [18] M. Vallet-Regi, F. Balas, M. Colilla, M. Manzano, *Bioceramics and pharmaceuticals: a remarkable synergy*, *Bioceramics and pharmaceuticals*, *Solid State Sci.* 9 (2007) 768–776.
- [19] Sh. Kapoor, R. Hegde, A.J. Bhattacharyya, Influence of surface chemistry of mesoporous alumina with wide pore distribution on controlled drug release, *J. Control. Release* 140 (2009) 34–39.
- [20] Sh. Guo, D. Li, L. Zhang, J. Li, E. Wang, Monodisperse mesoporous superparamagnetic single-crystal magnetite nanoparticles for drug delivery, *Biomaterials* 30 (2009) 1881–1889.
- [21] Q. Tang, Y. Xu, D. Wu, Y. Sun, A study of carboxylic-modified mesoporous silica in controlled delivery for drug famotidine, *J. Solid State Chem* 179 (2006) 1513–1520.
- [22] Q. Tang, Yuxi Chen, Jianghua Chen, J. Li, Y. Xu, D. Wub, Y. Sun, A study of carboxylic-modified mesoporous silica in controlled delivery for drug famotidine, *J. Solid State Chem.* 183 (2010) 76–83.
- [23] J.M. Rosenholm, M. Lindén, Towards establishing structure–activity relationships for mesoporous silica in drug delivery applications, *J. Control. Release* 128 (2008) 157–164.
- [24] A. Ramila, B. Munoz, J. Perez-Pariente, M. Vallet-Regi, Mesoporous MCM-41 as drug host system, *J. Sol-Gel Sci. Technol.* 26 (2003) 1199–1202.
- [25] Sh.K. Das, Sh. Kapoor, H. Yamada, A.J. Bhattacharyya, Effect of surface acidity and pore size of mesoporous alumina on degree of loading and controlled release of ibuprofen, *Micropor. Mesopor. Mater.* 118 (2009) 267–272.
- [26] J. Anderson, J. Rozenholm, S. Areva, M. Linden, Influences of material characteristics on ibuprofen drug loading and release profiles from ordered micro- and mesoporous silica materials, *Chem. Mater.* 16 (2004) 4160–4167.
- [27] T. Heikkila, J. Salonen, J. Tuura, M.S. Hamdy, G. Mul, N. Kumar, T. Salmi, D.Yu. Murzin, L. Laitinen, A.M. Kaukonen, J. Hirvonen, V.-P. Lehto, Mesoporous silica material TUD-1 as a drug delivery system, *Int. J. Pharma.* 331 (2007) 133–138.
- [28] Y. Zhu, J. Shi, Y. Li, H. Chen, W. Shen, X. Dong, Storage and release of ibuprofen drug molecules in hollow mesoporous silica spheres with modified pore surface, *Micropor. Mesopor. Mater.* 85 (2005) 75–81.
- [29] Y.-J. Yang, X. Tao, Q. Hou, J.-F. Chen, Fluorescent mesoporous silica nanotubes incorporating CdS quantum dots for controlled release of ibuprofen, *Acta Biomater.* 5 (2009) 3488–3496.
- [30] Brian G. Trewyn, Igor I. Slowing, Supratim Giri, Hung-Ting Chen, Victor S.-Y. Lin, Synthesis and functionalization of a mesoporous silica nanoparticle based on the sol-gel Process and applications in controlled release, *Acc. Chem. Res.* 40 (9) (2007) 846–853.
- [31] I.B. Lenor, E.T. Baran, M. Kawashita, R.L. Ries, T. Kokubo, T. Nakamura, Growth of a bonelike apatite on chitosan microparticles after a calcium silicate treatment, *Acta Biomater.* 4 (2008) 1349–1359.
- [32] M. Grün, K.K. Unger, A. Matsumoto, K. Tsutsumi, Novel pathways for the preparation of mesoporous MCM-41 materials: control of porosity and morphology, *Micropor. Mesopor. Mater.* 27 (1998) 207–216.
- [33] S. Huh, J.W. Wiench, J.-Ch Yoo, M. Pruski, V.S.-Y. Lin, Organic functionalization and morphology control of mesoporous silicas via a co-condensation synthesis method, *Chem. Mater.* 15 (2003) 4247–4256.
- [34] A. Katiyar, S. Yadav, P.G. Smirniotis, N.G. Pinto, Synthesis of ordered large pore SBA-15 spherical particles for adsorption of biomolecules, *J. Chromatogra. A* 1122 (2006) 13–20.
- [35] O.I. Lebedev, G. Tandeloo, C. Thoelen, W. Rhijn, P.A. Jacobs, *Adv. Mater.* 13 (2001) 1317.
- [36] Sh. Xing Wang, Y. Zhou, W. Guan, B. Ding, Preparation and characterization of stimuli-responsive magnetic, nanoparticles, *Nanoscale Res. Lett.* 3 (2008) 289–294.
- [37] L. Vradman, L. Titelman, M. Herskowitz, Size effect on SBA-15 microporosity, *Micropor. Mesopor. Mater.* 93 (2006) 313–317.
- [38] A. Galarneau, H. Cambon, F. Di Renzo, R. Ryoo, M. Choi, F. Fajula, Microporosity and connections between pores in SBA-15 mesostructured silicas as a function of the temperature of synthesis, *New J. Chem.* 27 (2003) 73–79.